IDEAL SHEAR STRENGTHS AND BOND DIRECTIONALITY OF FCC and BCC METALS

S.Ogata[1], J.Li[2], Y.Shibutani[1], and S.Yip[3]

[1] Department of Mechanical Engineering and Systems,
Handai Frontier Research Center, Osaka University, Osaka 565-0871, JAPAN
[2] Department of Materials Science and Engineering,
Ohio State University, Columbus, OH 43210, USA
[3] Department of Nuclear Engineering, Department of Materials Science and Engineering,
Massachusetts Institute of Technology, Cambridge, MA 02139, USA

ABSTRACT

We calculate the ideal pure shear strengths of FCC Al, Cu, Ni and BCC W, Mo, Fe in their common slip systems using density functional theory (DFT). We find the critical shear strains (CSS) of BCC metals are narrowly distributed (~ 0.18), and are higher than those of FCC metals except Al. In contrast, the CSS of FCC metals spread over a wide range ($0.137 \sim 0.2$), with Al having extremely high CSS (~ 0.2). By comparative analyses of valence charge distributions, we argue that FCC Al and BCC metals have strong directional bonding, and ferromagnetic Ni have moderate and Cu have weak directional bonding.

1. INTRODUCTION

Ideal strength, which can be defined as the stress necessary to induce permanent deformation in a material without prior imperfections[1, 2, 3, 4, 5, 6, 7], is one of the important materials characterizations. With the possible exception of recent nanoindentation measurements [8, 9, 10], it has not been feasible to directly measure the ideal shear strength of materials. Ogata *et al.* [11] performed DFT calculations for Al and Cu perfect single crystal, and found Al has higher ideal pure shear strength than Cu, because Al has relatively strong bond directionality, and the bond directionality induces higher CSS, and then higher ideal shear strength.

Here we estimate ideal shear strength and CSS of FCC Al, Cu, Ni and BCC Mo, W, Fe, and perform valence charge distribution analyses of these metals to discuss the bond directionality of metals.

2. METHOD

We used the Vienna Ab-initio Simulation Package (VASP) [12, 13] for DFT calculations under shear deformations. The exchange-correlation density functional adopted is Perdew-Wang generalized gradient approximation (GGA) [14]. Ultrasoft (US) pseudopotentials [17] are used for the FCC metals and BCC Mo and W, and the projector augmented-wave (PAW) method [18] for the BCC Fe. Brillouin zone (BZ) k-point sampling is performed using the Monkhorst-Pack Algorithm[19]. BZ integration follows the Methfessel-Paxton scheme [20] with the smearing width chosen so the entropic free energy ("$-TS$" term) is less than 0.5 meV/atom.

Incremental affine shear strains are imposed on each crystal along the common slip systems to obtain the corresponding unrelaxed and relaxed stresses. The unrelax and relax conditions are defined by ϵ_{ij}=0 excluding $\gamma \equiv x/d_0$ (d_0 is the equilibrium separation between two adjacent atomic planes and x is the shear displacement along the Burgers vector, b) and σ_{ij}=0 excluding the resolved shear stress, respectively.

Table 1: Ideal $\{111\}\langle 11\bar{2}\rangle$ shear strains and stresses of Al, Ni and Cu. γ_m^0 is the ideal shear strain of Frenkel's model.

	relaxed				unrelaxed			
material	γ_m^r	γ_m^r/γ_m^0	σ_m^r GPa	σ_m^r/G_r	γ_m^u	γ_m^u/γ_m^0	σ_m^u GPa	σ_m^u/G_u
Al	0.200	1.13	2.84	0.110	0.210	1.19	3.73	0.147
Ni	0.140	0.79	5.05	0.084	0.160	0.91	6.29	0.079
Cu	0.137	0.77	2.16	0.070	0.157	0.89	3.45	0.084

Table 2: Ideal shear strains and stresses of W, Mo and Fe.

	relaxed			unrelaxed		
material	γ_m^r	σ_m^r GPa	σ_m^r/G_r	γ_m^u	σ_m^u GPa	σ_m^u/G_u
W $\{110\}\langle\bar{1}\bar{1}1\rangle$	0.179	17.52	0.114	0.196	17.63	0.113
W $\{211\}\langle\bar{1}\bar{1}1\rangle$	0.176	17.37	0.113	0.175	17.28	0.111
W $\{321\}\langle\bar{1}11\rangle$	0.176	17.33	0.113	0.175	17.27	0.111
Mo $\{110\}\langle\bar{1}11\rangle$	0.190	15.18	0.120	0.192	16.52	0.123
Mo $\{211\}\langle\bar{1}\bar{1}1\rangle$	0.175	14.84	0.117	0.177	15.99	0.119
Mo $\{321\}\langle\bar{1}\bar{1}1\rangle$	0.176	14.87	0.117	0.175	15.93	0.119
Fe $\{110\}\langle\bar{1}\bar{1}1\rangle$	0.178	8.14	0.106	0.234	11.43	0.142
Fe $\{211\}\langle\bar{1}\bar{1}1\rangle$	0.184	7.51	0.099	0.236	9.95	0.124
Fe $\{321\}\langle\bar{1}11\rangle$	0.181	7.57	0.100	0.197	9.43	0.118

3. RESULTS AND DISCUSSIONS

At equilibrium, Cu is considerably stiffer than Al, with simple and pure shear moduli greater by 65% and 25%, respectively, than Al. However, Al ends up with 70% and 32% larger ideal pure shear strength σ_m^r than Cu, respectively, because it has a longer range of strain before softening: γ_m=0.200 in Al and γ_m=0.137 in Cu. The σ_m^r/G_m^r ratio shows a similar trend the two are in fact almost linearly correlated (see Table 1).

BCC metals have three common slip systems which are almost equally likely. We performed the same shear deformation calculations in the three slip systems as for fcc metals. The ideal shear strains are rather narrowly distributed (~ 0.18)[25] and in good agreement with the previous Mo result [26]. Moreover, the values of σ_m^r/G_m^r for the three metals are almost equal (~ 0.11) and are also close to that of Al (Table. 2). This suggests that the BCC metals have more bond directionality than the FCC metals except Al.

Figs. 1, 2 shows the iso-surfaces of valence charge density ($h \equiv V_{\rm cell}\rho_{\rm v}$, $V_{\rm cell}$ and ρ_v are the supercell volume and valence charge density, respectively) of the FCC and BCC metals. We select two h-contour values for each metal, and for Ni (FM) the difference between spin-up and -down densities ($h_{\text{diff}} \equiv V_{\text{cell}}(\rho_{\text{v}} \uparrow - \rho_{\text{v}} \downarrow)$) is also shown. At the octahedral interstice in Al (Fig.1(a)), the pocket of charge density has cubic symmetry and is angular in shape, with a volume comparable to the pocket centered on every ion. In contrast, Figs. 1(c), 1(d), show that in Cu there is no such interstitial charge pocket, the charge density being nearly spherical about each ion. Al has an inhomogeneous charge distribution in the interstitial region because of bond covalency [21] and directional bonding [22], while Cu have relatively homogeneous charge distributions and little bond directionality. For Ni, the total charge density (spin-up plus -down) shows a spherical distribution (Fig.1(e),1(f)). However, the difference between spin-up and -down (1(h)), which results in magnetization, shows a cube-shaped distribution centered on the ion, similar to that in Al (Fig.1(b)), even though the volume is smaller. This suggests that magnetization promotes directional bonding and causes the γ_m, σ_m^r/G_m^r values of Ni to deviate from those of Cu. In BCC W and Mo, we see cuboidal distortions of the ion-centered charge density which can be used to explain the bond directionality. In Fe, the total charge density (spin-up plus spin-down) is almost spherical. However, the difference between spin-up and spin-down (Fig. 2(h)) clearly shows angular distortion as well. This agrees with the general observation that magnetism is important for phase stability and elasticity [27]; it is responsible for stabilizing the bcc phase of Fe at ambient conditions which would otherwise take a close-packed structure.

References

[1] Wang J., Li J., Yip S., Phillpot S., and Wolf D. (1995) *Phys. Rev.* B **52**, 12627.

[2] Roundy, D. and Krenn, C. R. and Cohen, M. L. and Morris, Jr., J. W. (1999) *Phys. Rev. Lett.* **82**, 2713.

[3] Morris, J. W. and Krenn, C. R. (2000) *Phil. Mag.* A **80**, 2827.

[4] Krenn, C. R., Roundy, D., Morris, J. W. and Cohen, M. L. (2001) *Mater. Sci. Eng.* A **319**, 111.

[5] Roundy, D., Krenn, C. R., Cohen, M. L. and Morris, J. W. (2001) *Phil. Mag.* A **81**, 1725.

[6] Černy, M., Pokluda J., Šob, M., Friák, M., Šandera, P. (2003) *Phys. Rev.* B **67**, 035116.

[7] Šob, M. and Friák, M. and Legut, D. and Vitek, V. (2003) *Psi-k Bulletin*, **58**, 130.

[8] Gouldstone A., Koh H.J., Zeng K.Y., Giannakopoulos A.E., and Suresh S. (2000) *Acta Mat.* **48**, 2277.

[9] Li J., Van Vliet K.J., Zhu T., Yip S., and Suresh S. (2002) *Nature* **418**, 307.

[10] Van Vliet K.J., Li J., Zhu T., Yip S., and Suresh S. (2003) *Phys. Rev.* B **67**, 104105.

[11] Ogata S., Li J., and Yip S. (2002) *Science* **298**, 807.

[12] Vienna Ab-initio Simulation Package: Kresse G. and Hafner J. (1993) *Phys. Rev.* B **47**, RC558.

[13] Kresse G. and Furthmuller J. (1996) *Phys. Rev.* B **54**, 11169.

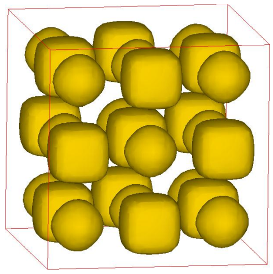
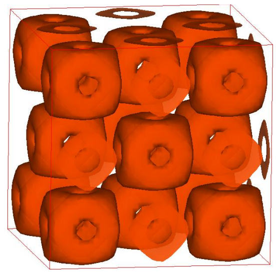

(a) Al ($h = 2.89$) (b) Al ($h = 3.36$)

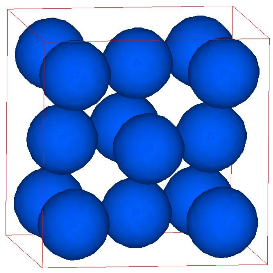
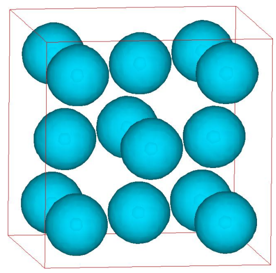

(c) Cu ($h = 9.00$) (d) Cu ($h = 20.00$)


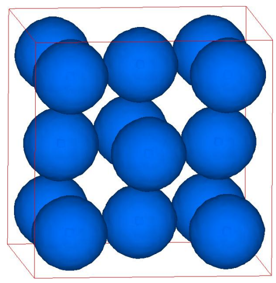

(e) Ni ($h = 3.66$) (f) Ni ($h = 8.99$)

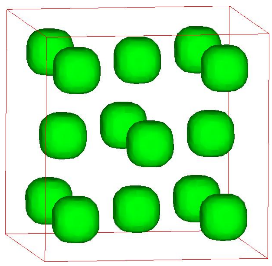
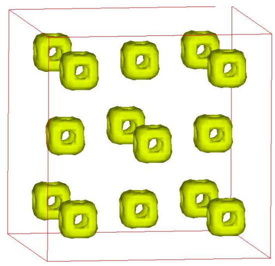

(g) Ni ($h_{\mathrm{diff}} = 4.0$) (h) Ni ($h_{\mathrm{diff}} = 6.0$)

Figure 1: Valence charge density iso-surfaces in FCC metals.

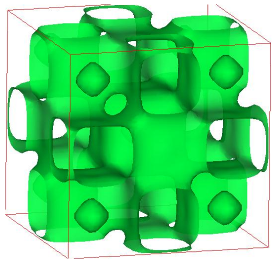

(a) W ($h = 5.64$)

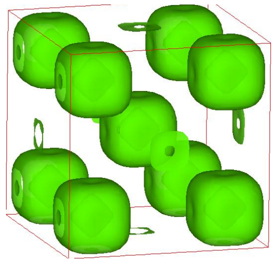

(b) W ($h = 7.63$)

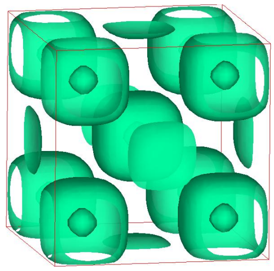

(c) Mo ($h = 5.80$)

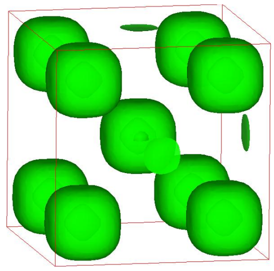

(d) Mo ($h = 8.60$)

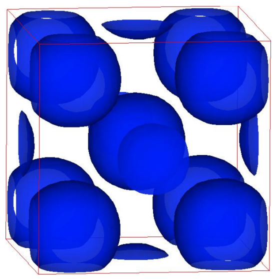

(e) Fe ($h = 5.00$)

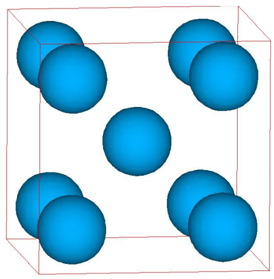

(f) Fe ($h = 18.00$)

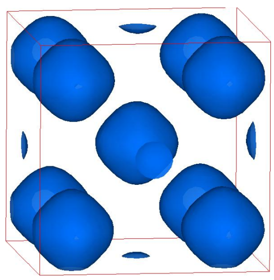

(g) Fe ($h_{\mathrm{diff}} = 5.00$)

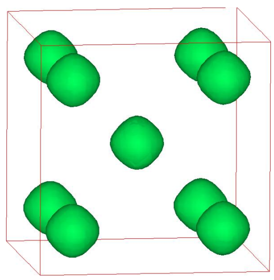

(h) Fe ($h_{\mathrm{diff}} = 18.00$)

Figure 2: Valence charge density iso-surfaces in BCC metals.

[14] Perdew J.P. and Wang Y. (1992) *Phys. Rev.* B **46**, 6671.

[15] Ceperley, D. and Alder, B.J. (1980) *Phys. Rev. Lett.* **45**, 566.

[16] Perdew, J.P. and Zunger, A. (1981) *Phys. Rev.* B **23**, 5048.

[17] Vanderbilt, D. (1990) *Phys. Rev.* B **41**, 7892.

[18] Kresse, G. and Joubert, J. (1999) *Phys. Rev.* B **59**, 1758-75.

[19] Monkhorst, H.J. and Pack, J.D. (1976) *Phys. Rev.* B **13**, 5188.

[20] Methfessel, M. and Paxton, A.T. (1989) *Phys. Rev.* B **40**, 3616-21.

[21] Feibelman P.J. (1990) *Phys. Rev. Lett.* **65**, 729.

[22] Grossman J.C., Mizel A., Cote M., and Cohen M.L., Louie S.G. (1999) *Phys. Rev.* B **60**, 6343.

[23] Zimmerman J.A., Gao H., Abraham F.F. (2000) *Model. Simul. Mater. Sci. Eng.* **8**, 103.

[24] Rice J.R. and Beltz G.E. (1994) *J. Mech. Phys. Solids* **42**, 333.

[25] Paxton A.T., Gumbsch P., Methfessel M. (1991) *Phil. Mag. Lett.* **63**, 267.

[26] Luo W., Roundy D., Cohen M.L., and Morris J.W. (2002) *Phys. Rev.* B **66**, 094110.

[27] Cohen R.E., Gramsch S., Steinle-Neumann G., and Stixrude L. (2002) *Proceedings of the International School of Physics "Enrico Fermi"*, Volume CXLVII, *High-Pressure Phenomena*, eds. R.J. Hemley *et al.*.
`cond-mat/0110025`.